UDC 669.017:539.16

APPLICATION OF HYDROGEN EMBRITLEMENT MODELS TO THE BLISTER GROWTH BEHAVIOR IN 12Cr2MoNbVB STEEL AND α-Fe EXPOSED TO LOW-ENERGY D PLASMA

A.V. Nikitin, G.D. Tolstolutskaya, V.V. Ruzhytskiy, I.E. Kopanets, S.A. Karpov, R.L. Vasilenko, G.Y. Rostova, N.D. Rybalchenko, B.S. Sungurov
Institute of Solid State Physics, Material Science and Technology NSC KIPT, Kharkov, Ukraine

Processes of blisters and associated subsurface cracks nucleation during exposure of 12Cr2MoNbVB ferritic-martensitic steel and α-Fe under glow discharge hydrogen (deuterium) plasma with ion energies of ~ 1 keV and ion fluencies up to $2\cdot10^{24}$ D/м^2 at various temperatures have been examined. The methods used were scanning electron microscopy, thermal desorption spectroscopy and the D(^{3}He, p)^{4}He nuclear reaction. Temperature dependence of average blister diameter, the deuterium depth distribution and retention were studied. Application of hydrogen induced cracking models was considered to assess the effects of hydrogen from the plasma on the development of blisters and subsurface cracks. Based on this analysis, it is shown that significant crack growth rates can occur during reactor shut-down periods when the temperature of the structure decreases to less than about 373 K.

INTRODUCTION

The problem of materials selection for the vacuum chamber and protection of the chamber from the fusion plasma exposure is one of the most important in the creation and design of fusion devices [1, 2]. One of the most promising structural materials for nuclear fusion reactors is ferritic-martensitic steel with a low activation in a fusion neutron spectrum [3]. Despite the fact that steel is rarely considered as the plasma facing material due to the high sputtering coefficient, low thermal conductivity and high atomic number of constituting elements, adversely affecting the plasma, in recent years, some authors discussed the use of plasma facing elements made of steel without additional protection [4, 5]. For example, steel is used in some places of tokomak ASDEX-U central column as the plasma facing material [6]. In addition, the impact of thermonuclear plasma on the steel is possible in some areas that are not protected with additional elements, such as nozzles in a vacuum fusion reactor chamber, as well as for technological discharges.

Ferritic-martensitic steels are known to be particularly susceptible to nucleation of both blisters and associated subsurface cracks arising during exposure to glow discharge hydrogen plasma with ion energies of ~ 1 keV [7–10]. Such low ion energies are known to be characteristic of near-wall plasma fluxes in fusion reactors [11].

The Fe-H system has been the subject of many thermodynamic and kinetic researches on interstitial solute because of the high hydrogen diffusivity in iron. To understand hydrogen embrittlement of steel, many studies on the role hydrogen on properties of steel have been carried out [12]. Hydrogen induced crack growth in materials can result from both external gaseous or cathodic hydrogen and from internal dissolved hydrogen. In a fusion reactor there are several potential sources of hydrogen or hydrogen isotopes including direct injection from the plasma, tritium gas in the breeding blanket, nuclear (n, p) reactions within the material etc [12].

Hydrogen has been shown to induce cracking in a wide variety of materials, including ferritic steels, austenitic stainless steels, nickel-based alloys and aluminum alloys. The mechanism by which hydrogen causes cracking is generally thought to be the collection of hydrogen atoms at particle-matrix interfaces, grain boundaries and ahead of the crack tip or other defects.

Temperature and hydrogen activity are two parameters on which the crack growth rate is strongly dependent. Material parameters such as yield strength, hydrogen diffusivity, hydrogen trap densities and strength, and grain boundary chemistry are also important.

The purpose of this paper is to use existing models of hydrogen induced crack (HIC) growth to development of blisters and subsurface cracks in 12Cr2MoNbVB ferritic-martensitic steel and α-Fe exposed to glow discharge deuterium plasma with energy of ~ 1 keV at ion fluencies up to ~ $2\cdot10^{24}$ D/m^2.

1. MATERIAL AND METHODS

The materials used were 12Cr2MoNbVB (EP-450) ferritic-martensitic steel and α-Fe. The chemical composition of the steel was 0.118C-12Cr-0.28Ni-0.26Mn-1.41Mo-0.46Nb-0.21V-0.21Si-0.034P-0.004S with balance iron, all in weight %. The heat treatment of EP-450 consisted of quenching from 1323 K (1050 °C), followed by tempering at 1013 K (740 °C) for 1 h. The microstructure of the EP-450 alloy at this point consisted of a duplex structure of ferrite and tempered martensite at a volume ratio of approximately 1:1. Large globular $M_{23}C_6$ carbides were observed along both ferrite-ferrite and ferrite-tempered martensite grain boundaries. Disks with diameter of 18 mm were cut from a sheet with thickness of 2.4 mm.

The samples of α-Fe (bcc) with a purity of 99.9 wt.% were annealing at 1600 K after rolling and cutting. It contains impurities of more than a dozen elements. The carbon and copper concentration are of about 0.02 and 0.1%, respectively. The remaining elements are in thousandths of a percent. The specimens

with dimensions of 10×7 mm were cut from a sheet with thickness of 1 mm.

The surface of each sample was polished mechanically and then electropolished in a standard electrolyte to remove any mechanically damaged near-surface layer.

Several experiments were performed on the samples that were deformed at deformation levels in the range of 80…95%. Deformation was carried out by cold working via rolling at room temperature.

The specimens were irradiated at various temperatures with deuterium ions using glow gas-discharge plasma electrodes at 1000 V, producing an ion flux of 10^{19} H(D)/(m^2·s). In this study we chose D instead H in order to easily measure the depth dependence of the implanted and diffused hydrogen. The maximum irradiation fluence was $2\cdot10^{24}$ D/m^2.

The temperature during plasma exposure was varied between 240 and 400 K. The specimen was placed in a resistively-heated holder. The target temperature was continuously monitored using a thermocouple in the base of the specimen holder and was attached to the lower surface of specimen. Temperature maintenance on the steel samples in this device was achieved either by resistive heating or liquid nitrogen cooling. The temperature was maintained to within ±2.5 K. A detailed schematic diagram of the experimental setup is presented in Ref. [13].

The D concentration in the plasma-exposed samples was measured by means of the D(^{3}He, α)H reaction, where protons were analyzed. To determine the D concentration at larger depths, an analyzing beam of ^{3}He ions with energies varied from 0.3 to 1.4 MeV was used. The proton yields measured at different ^{3}He ion energies allow measuring the D depth profile at depths of up to 2 μm.

Total deuterium retention in the samples was monitored ex-situ using thermal desorption spectrometry (TDS). A resistive heater was used to heat the samples at a ramp rate of 6 K/s and the sample temperature was raised to 1300 K. D_2 molecules released during TDS run were monitored by monopole mass spectrometer.

A JEOL JSM-7001F 00 scanning electron microscope was used to study the surface morphology. Investigations of surface microstructure were performed using a MMO-1600-AT metallographic microscope.

2. RESULTS AND DISCUSSION

The influence of irradiation fluence on the kinetics of blister growth at 273 K on surface of 12Cr2MoNbVB steel is shown in Fig. 1. This temperature was chosen based on the temperature dependence data of the blistering processes on this steel [10, 13]. It is seen that for fluencies $(1…5)\cdot10^{23}$ m^{-2} the mean diameter and density of blisters increases monotonically with increasing fluence and then the growth of blisters stops.

Based on these results, the investigations of all blisters characteristics were performed in the dose saturation area.

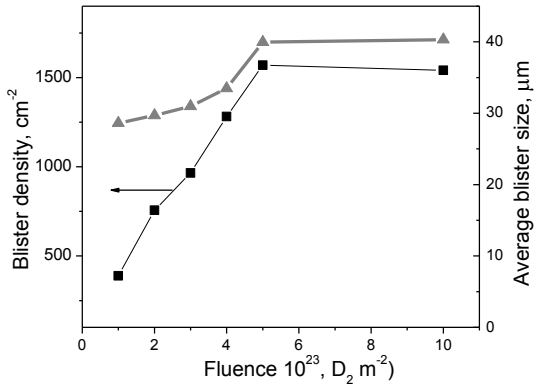

Fig. 1. Fluence dependence at temperature 273 K of kinetics of blister growth during hydrogen plasma exposure of 12Cr2MoNbVB steel

Fig. 2 shows the temperature dependence of average diameters and density of blisters (ρ) formed under deuterium plasma on the surface of 12Cr2MoNbVB steel and α-Fe.

The temperature dependence of mean blister diameter has a clearly expressed maximum at 283 and 250 K for steel and α-Fe, respectively. The density of blisters at temperatures 220…260 K does not change substantially, and then decreases. The specific temperature bounds for α-Fe shifted to lower temperatures compared to steel.

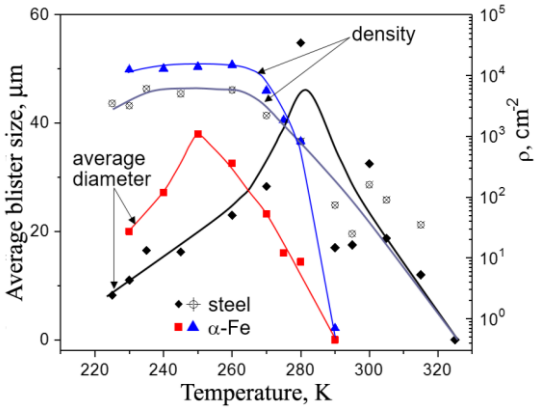

Fig. 2. Temperature dependence of average diameter and density of blisters formed under deuterium plasma irradiation to $1\cdot10^{24}$ D/m^2 for 12Cr2MoNbVB steel and α-Fe

It was mentioned in the introduction that the emergence of blisters associated with underground fissures. Various aspects of hydrogen induce cracking in a wide variety of materials were considered by several authors [14]. The observations of crack growth of high-strength steel in gaseous embrittling hydrogen have been done [14–16]. Modeled the crack growth rate-temperature dependence of HT-9 steel were found. The examples of the two types of curves of crack growth rate versus temperature are given in Fig. 3. The specific features of the crack growth due to different yield strength effects ($\sigma_{ys1} < \sigma_{ys2}$) are presented also. As can be seen from Fig. 3 the temperature of rapid decline of the crack growth rate is decreased with decreasing of yield strength.

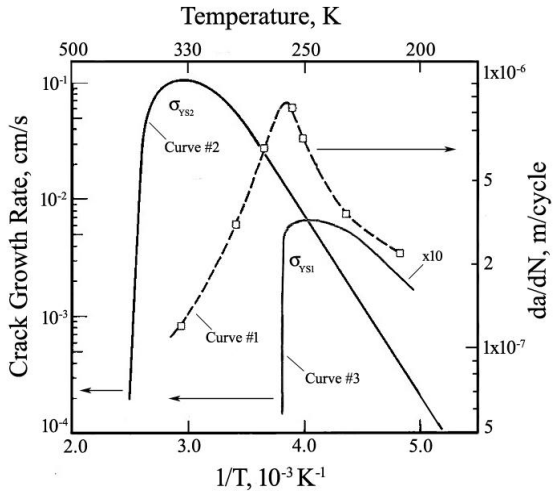

Fig. 3. Calculated dependence of crack growth vs reciprocal temperature for steels in low pressure hydrogen: curves #1 [17], #2 [12], and #3 [18]

The dependence of the crack growth rate *da/dt* could be described by the following hydrogen adsorption isotherm for the low-temperature regime (curve #1), eq. (1), and the high-temperature regime (curve #1), eq. (2), in Fig. 3:

$$\frac{da}{dt} = C_3 P^{1/2} \exp(-E_m/RT), \quad (1)$$

$$\frac{da}{dt} = C_4 P^{3/2} T^{-1/2} \exp[-(\Delta H + E_m)/RT)], \quad (2)$$

where P is the hydrogen partial pressure; E_m – the energy of migration of an atom from an initial physisorption site to a final chemisorption site; R is the gas constant and T is the temperature. C_3 and C_4 are constants, and ΔH is the heat of adsorption of hydrogen [12, 19].

Eqs. (1) and (2) are appropriate for assessing the crack growth rates of a fusion reactor first wall exposed to a hydrogen gas. To adopt them for evaluating the effect of hydrogen plasma on the crack growth rate it is necessary to relate the hydrogen flux impinging on a first wall to an equivalent hydrogen gas pressure which would give the same collision rate with the surface. Such a comparison has been made by Ashby [20] where hydrogen flux of 10^{17} H/(cm^2·s) was equal to a pressure of 10^{-2} Pa. This pressure was used to represent the effect of hydrogen plasma on the crack growth rate of HT-9 as a first estimate. It is clear from this calculation that the hydrogen activity of the plasma is sufficiently low as to have no effect on the crack growth rate of HT-9 based on this analysis. The maximum crack growth calculated with eqs. (1) and (2) for a pressure of 10^{-2} Pa is $1.6 \cdot 10^{-9}$ cm/s, and it occurs at a temperature of 148 K. At 298 K the crack growth rate is 10^{-13}, and at 573 K it is 10^{-15} cm/s. However if it taken into account the hydrogen concentration in a fusion first wall structure made of HT-9 for various surface reactions and for conditions of hydrogen generation by (*n, p*) reaction and direct injection from the plasma a crack growth rate of 10^{-1} cm/s was estimated for this condition at a temperature of 348 K [12]. In this way, significant crack growth rates will be feasible in atomic hydrogen at temperatures up to 370 K (see curve #2, Fig. 3).

Comparison of the curves shown in Figs. 2 and 3 demonstrates correlation between temperature ranges of embrittlement and blistering. Taking into account that blister diameter defines the linear dimension of associated subsurface crack, and the latter is accepted as a characteristic of crack growth rate, the dependence of average blisters size on the temperature seems in good agreement with theoretical predictions. Some scatter of points at temperatures 290…300 K for steel EP-450 assumes the existence of the second maximum. The reliability of this two-peak phenomenon requires additional investigation.

The kinetics of hydrogen assisted crack growth in high-strength steels are governed by the combined effects of chemical and mechanical driving forces, and relate to the individual processes involved in the transport of hydrogen from the gas phase to the point of fracture and to the embrittlement process at the fracture process zone (FPZ). The embrittlement process is expected to depend on both hydrogen concentration and tensile stress level in the FPZ. Models based on the critical role of stress in gaseous hydrogen embrittlement suggested that the FPZ can be either at the crack tip (surface) or at some distance away from the crack tip (bulk). On the other hand, it may be more reasonable to assume that the location of the FPZ is determined by hydrogen segregation at specific microstructural features in the near surface region. Theoretical and experimental results indicate that hydrogen segregation (several orders of magnitude higher than the lattice solubility) can occur at trap sites; such as, grain boundaries, voids, second phase boundaries and dislocations.

The physical model of hydrogen blister nucleation in metals is predicted that dissolved hydrogen atoms can aggregate into a vacancy-hydrogen cluster. The hydrogen atoms in this cluster become hydrogen molecules that can stabilize the cluster (small cavity) [21]. The cluster will grow preferentially in the sites of stress concentration because of high hydrogen concentration. When the blister nucleus grows to a critical size C_{cr} and the stress concentration equates to the atomic binding force, which may be decreased by hydrogen, cracks will initiate from the wall of the cavity due to the internal hydrogen pressure. In a recently published paper [22], it was shown that most of the hydrogen blisters initiate from grain boundaries or matrix interface and inclusion or second phase particles. The cohesive strength of interface is much lower than that of the matrix. Cracks are easy to initiate on interface and propagate. Therefore, the probability of initiation of hydrogen blisters on grain boundary and interface of second phase and matrix is higher than that in matrix.

Thus, since hydrogen activity is one of the key parameters that determine the crack growth rate, it is necessary to clarify the hydrogen retention and transport behavior in investigated steel and α-Fe.

The trapping of deuterium by defects represent the data obtained by TDS. Fig. 4 shows desorption profiles of deuterium from α-Fe exposed to deuterium plasma at 283 K and ion implanted at 90 K.

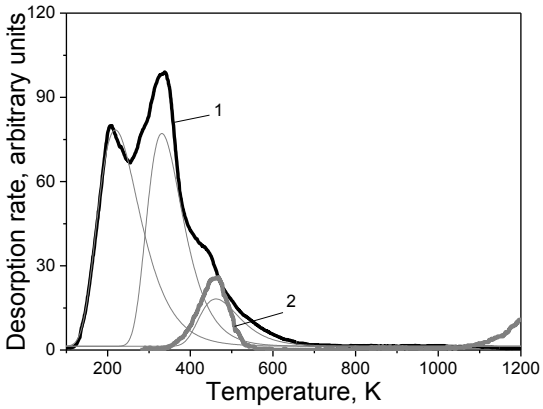

Fig. 4. Thermal desorption spectra of D from α-Fe ion implanted at 90 K to a dose of $1 \cdot 10^{21}$ D/m^2 (1) and exposed to deuterium plasma at 283 K to $1 \cdot 10^{24}$ D/m^2 (2)

In the case of plasma exposure, the release of deuterium from iron sample starts at ~ 330 K. The maximum of desorption peak is observed at 470 K. The decreasing of temperature of the exposure during ion implantation led to complication of the TD spectra. In addition, the increasing of deuterium retention (in comparison with the 283 K case) was found. Thus, the temperature interval of blister nucleation and growth correlates with the temperatures corresponding to strong hydrogen trapping in α-Fe (see Figs. 2, 4).

To understand the hydrogen transport behavior in steel and α-Fe the depth profiling is critically important. Fig. 5 presents the depth distribution profiles of deuterium in 12Cr2MoNbVB steel exposed to 1 keV deuterium plasma to $1 \cdot 10^{24}$ D/m^2 at room temperature.

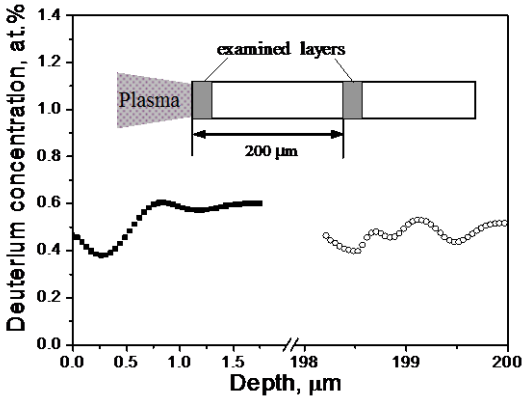

Fig. 5. Distribution profiles of deuterium in 13Cr2MoNbVB steel exposed to deuterium plasma at 300 K to a dose of $2 \cdot 10^{24}$ D/m^2 at a depth of 0…1.8 (■) and ~ 200 μm (○) from irradiated surface

Initially, measurements were carried out on the plasma-exposed surface of the specimen, and then after removing of material by electropolishing, measurements were continued at the depths starting at 200 μm from the front surface. An essentially uniform distribution of deuterium within the range 0…200 μm with an average concentration of ~ 0.5 at.% has been observed.

The calculated normal-incident range of 0.5 keV D^+ in iron is about 7 nm. Detection of deuterium at a depth of 200 μm confirms that the implanted D migrates into the bulk far beyond the ion range and thereby can promote nucleation of cavities and cracks at this depth.

Structural alloys are beginning to serve in various initial metallurgical states depending on the mechanical treatment (forging, rolling or drawing), and thermal history (intermediate annealing and final hardening stories) that were used during their production. It is anticipated that the structural-phase state of the near-surface region of a specific alloy can affect the various processes of erosion.

Figs. 6, 7 show surface morphologies and microstructures of recrystallized and 80% deformed specimens of α-Fe after irradiation to a fluence of $2 \cdot 10^{24}$ D/m^2 at 273 K.

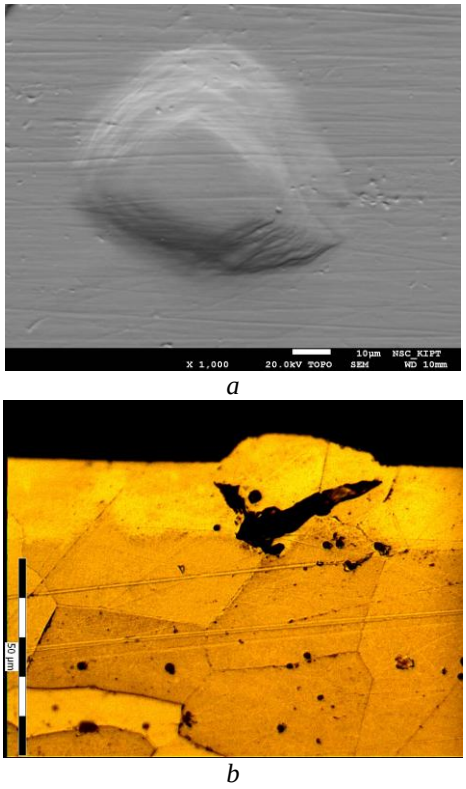

a

b

Fig. 6. Surface morphology (a) and microstructure of cross-section of recrystallized α-Fe samples after irradiation with deuterium plasma to $2 \cdot 10^{24}$ D/m^2 at 273 K (b)

For recrystallized (RE) α-Fe the large blisters were observed with sizes of a few tens of micrometers and a shape of high dome. These blisters showed a multi-layered structure like steps (see Fig. 6,a). The microstructures of cross-section of recrystallized α-Fe samples had low elongation grains with a grain size of 50…100 μm.

In the case of pre-exposure deformation (PD) most of blisters had spherical-like shapes (see Fig. 7). The blister height and the blister size have a virtually constant relation: the height is more than one order of magnitude smaller than the blister size (see Fig. 7,a). This could be attributed to the microstructure of PD α-Fe, which layered with high elongation grains arranged parallel to the surface. Besides the layered structures were somewhat disordered. Some cracks were observed in grain boundaries (see Fig. 7,b). These

results indicate that structural state has a significant impact on the development of blistering and its parameters.

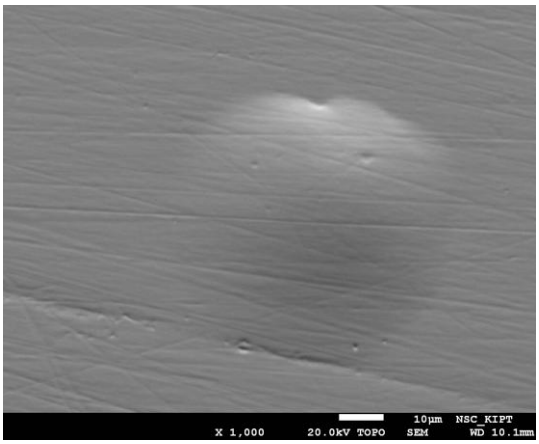

a

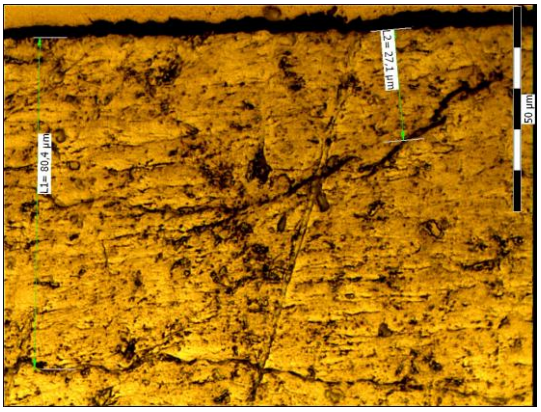

b

Fig. 7. Surface morphology (a) and microstructure of cross-section of 80% deformed α-Fe samples after irradiation with deuterium plasma to $2 \cdot 10^{24}$ D/m^2 at 273 K (b)

The blistering development is influenced not only by irradiation conditions, such ion energy, flux and fluence of incident H, subsurface microstructure and temperature of material but also the material yield strength. It is well known that the tensile strength is proportional to the hardness of material. The following Table shows Vickers hardness (load 50 g) for specimens having different structure.

Hardness of specimens

No.	Regime of treatment	Hardness, H_v^{50}, kG/mm^2
1	Recrystallized α-Fe	140…160
2	80 % deformed α-Fe	260…300
3	Cold working 95% EP-450	385…425
4	Stress relieved EP-450	270…300

Fig. 8 represents the dependence of blisters density on reciprocal temperature for 95% cold working and stress relieved 12Cr2MoNbVB steel and 80% deformed and recrystallized α-Fe under deuterium plasma irradiation to $2 \cdot 10^{24}$ D/m^2 at 273…350 K.

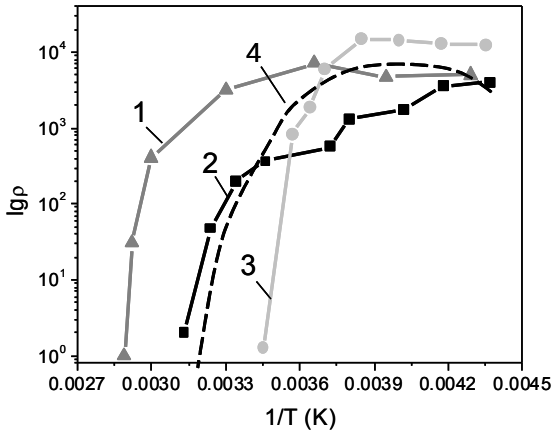

Fig. 8. Density of blisters – 1/T relationship for 12Cr2MoNbVB steel (1, 3) and α-Fe (2, 4) under deuterium plasma irradiation to $2 \cdot 10^{24}$ D/m^2 for cold working (1, 2) and stress-relieved (3, 4) states

Comparison of the data shown in Fig. 8 and Table reveals that an increase of hardness shifts the curves of blisters density to higher temperatures that in qualitative agreement with the model of crack growth of high-strength steel in gaseous embrittling hydrogen (see Fig. 3). It should be noted that the features of defect substructure caused by pre-exposure deformation are associated with a significant increase of the density of crack nucleation sites that may lead to a change of the mechanisms of hydrogen-related blistering.

Gerberich, Chen and St. John [15] have calculated the hydrogen-stress field interactions to develop a kinetic model of crack growth for internal hydrogen. They assumed that the crack growth kinetics which are nearly stress-intensity independent are controlled primarily by the plastic stress field. To account for strong hydrogen trapping, which is expected in HT-9, it is shown that the strong temperature dependence of this trapping could cause the crack velocity to decrease at higher temperatures.

Analysis of the temperature dependence of crack growth for internal hydrogen suggests that at temperatures exceeding about 323 K the crack growth rate decreases very rapidly to values that would be insignificant [15].

Alternate application of hydrogen induced cracking models to assess the possible effects of hydrogen from the plasma, nuclear reactions and cathodic corrosion has indicated that only internal hydrogen generated by nuclear reactions may potentially cause cracking at reactor operating temperatures. A crack growth rate of 60 cm/yr was calculated for a steady-state hydrogen concentration of 0.0005…0.5 appm at a temperature exceeding 473 K.

Experimental data obtained in this study indicate that development of blisters and associated subsurface cracks during exposure of 12Cr2MoNbVB ferritic-martensitic steel and α-Fe under glow discharge hydrogen (deuterium) plasma is observed up to temperature 350 K.

CONCLUSSIONS

Processes of blisters nucleation and associated subsurface cracks arising during exposure of 12Cr2MoNbVB ferritic-martensitic steel and α-Fe in glow discharge hydrogen (deuterium) plasma with ion energies of ~ 1 keV and ion fluencies of ~ $2 \cdot 10^{24}$ D/m^2 at various temperatures have been defined experimentally.

A close correlation of temperature ranges of hydrogen-induced blistering and theoretical predictions of HIC growth (hydrogen embrittlement) has been found.

The temperature interval of blister formation at a flux of 10^{19} H(D)/(m^2·s) depends on the retention and accumulation of large amounts of hydrogen.

Post-irradiation measurements of deuterium content showed that deuterium concentrations were relatively constant within investigated depth and extended far beyond the implantation range. Penetration of hydrogen to a greater depth confirms the development of cracks – embryos of blisters at depths on the orders of magnitude exceeding the range of hydrogen ions with energy 1 keV.

It is established that the initial state of EP-450 ferritic-martensitic steel and α-Fe has a strong influence on the development of blisters and crack formation under hydrogen plasma exposhure.

Significant crack growth rates could occur during reactor shut-down periods when the temperature of the structure decreases to less than about 373 K.

REFERENCES

1. G. Federici, C.H. Skinner, J.N. Brooks, J.P. Coad, C. Grisolia, A.A. Haasz, A. Hassanein, V. Philipps, C.S. Pitcher, J. Roth, W.R. Wampler, D.G. Whyte. Plasma-material interactions in current tokamaks and their implications for next step fusion reactors // *Nucl. Fusion.* 2001, v. 41, p. 1967-1981.

2. K. Tobita, S. Nishio, M. Enoeda, M. Sato, T. Isono, S. Sakurai, H. Nakamura, S. Sato, S. Suzuki, M. Ando, K. Ezato, T. Hayashi, T. Hirose, T. Inoue, Y. Kawamura, N. Koizumi, Y. Kudo, R. Kurihara, T. Kuroda, M. Matsukawa, K. Mouri, Y. Nakamura, M. Nishi, Y. Nomoto, J. Ohmori, N. Oyama, K. Sakamoto, T. Suzuki, M. Takechi, H. Tanigawa, K. Tsuchiya, D. Tsuru. Design study of fusion DEMO plant at JAERI // *Fusion Eng. Des*. 2006, v. 81, p. 1151-1158.

3. J. Roth, K. Sugiyama, V. Alimov, T. Höschen, M. Baldwin, R. Doerner. EUROFER as wall material: Reduced sputtering yields due to W surface enrichment // *J. Nucl. Mater.* 2014, v. 454, p. 1-6.

4. E. Herms, J.M. Olive, M. Puiggali. Hydrogen embrittlement of 316L type stainless steel // *Materisls Science and Engineering*. 1999, v. 272, N 2, p. 279-283.

5. M. Beghini, G. Benamati, L. Bertini, I. Ricapito, and R. Valentini. Effect of hydrogen on the ductility reduction of F82H martensitic steel after different heat treatments // *J. Nuclear Materials.* 2001, v. 288, p. 1-6.

6. I. Zammuto, L. Giannone, A. Houben, A. Herrmann, A. Kallenbach. Long term project in ASDEX upgrade: Implementation of ferritic steel as in vessel wall // *Fusion Eng. and Des*. (doi:10.1016 /j.fusengdes.2015.01.048).

7. Е.Д. Волков, Ю.А. Грибанов, И.М Неклюдов и др. Особенности эрозии поверхности стали Х13 при экспозиции в водородной плазме // *Вопросы атомной науки и техники. Серия «Физика радиационных повреждений и радиационное материаловедение»*. 1988, в. 5(47), с. 58-61.

8. В.И. Бендиков, А.В. Никитин, О.А. Опалев и др. Возникновение трещин в ферритной стали 12Х12М1БФР под действием потока ионов водорода // *Атомная энергия*. 1990, т. 68, в. 6, с. 406-408.

9. E. Shekari, M.R. Shishesaz, Gh. Rashed, M. Farzam, and E. Khayer. Failure Investigation of Hydrogen Blistering on Low-strength Carbon Steel. Iranian // *Journal of oil and Gas Science and Technology*. 2013, v. 2, N 2, p. 65-76.

10. А.В. Никитин, В.В. Ружицкий, И.М. Неклюдов, Г.Д. Толстолуцкая, И.Е. Копанец. Влияние деформации на возникновение трещин в стали Х13М2БФР под действием потока ионов водорода // *Вопросы атомной науки и техники. Серия «Физика радиационных повреждений и радиационное материаловедение»*. 2014, №2 (90), с. 34-38.

11. R.W. Conn, J. Kesner. Plasma modeling and first wall interaction phenomena in tokamaks // *J. Nucl. Mater.* 1976, v. 63, p. 1.

12. R.H. Jones. Application of hydrogen embrittlement models to the crack growth behavior of fusion reactor materials // *J. Nuclear Materials.* 1986, v. 141-143, p. 468-475.

13. A.V. Nikitin, G.D. Tolstolutskaya, V.V. Ruzhytskyi, V.N. Voyevodin, I.E. Kopanets, S.A. Karpov, R.L. Vasilenko, F.A. Garner. Blister formation on 13Cr2MoNbVB ferritic-martensitic steel exposed to hydrogen plasma // *J. of Nucl. Mater.* 2016, v. 478, p. 26-31.

14. *Gaseous hydrogen embrittlement of materials in energy technologies.* V. 2*: Mechanisms, modelling and future developments* / Edited by Richard P. Gangloff and Brian P. Somerday. Woodhead Publishing Limited, 2012, p. 500.

15. W.W. Gerberich, T. Livne, and X. Chen // *Proc. Symp. on Modeling Environmental Effects on Crack Initiation and Propagation*, Toronto, Canada, 1985 / Eds. R.H. Jones and W.W. Gerberich (TMS-AIME, Warrendale, PA).

16. D.P. Williams and H.G. Nelson. Embrittlement of 4130 steel by low-pressure gaseous hydrogen // *Metall. Trans.* 1970, v. 1, p. 63.

17. J.D. Frandsen and H.L. Marcus. Environmentally assisted fatigue crack propagation in steel // *Metallurgical transactions A.* 1977, v. 8a, p. 265-272.

18. R.P. Gangloff and R.P. Wei. Gaseous hydrogen embrittlement of high strength steels // *Metallurgical transactions A.* 1977, v. 8a, p. 1043-1053.

19. R.W. Pasco, K. Sieradzld, and P.J. Ficalora. A surface chemistry kinetic model of gaseous hydrogen embrittlement // *Scripta Metall*. 1982, v. 16, p. 881.

20. C. Ashby // *Proc. Third Topical Meeting on Fusion Reactor Materials*, Albuquerque, NM 1983 / Eds. J.B. Whitley, K.L. Wilson, and F.W. Clinard, Jr. North-Holland, Amsterdam, 1984, p. 1406.

21. X.C. Ren, Q.J. Zhou, G.B. Shan, W.Y. Cyu, J.X. Li, Y.J. SU, and L.J. Qiao. A Nucleation Mechanism of Hydrogen Blister in Metals and Alloys // *Metallyrgical and materials transactions*. 2008, v. 39A, p. 87-97.

22. Г.Д. Толстолуцкая, А.В. Никитин, В.В. Ружицкий, Н.Д. Рыбальченко, Р.Л. Василенко, И.М. Короткова. Развитие трещин в ферритной стали при облучении водородной плазмой // *Вопросы атомной науки и техники. Серия «Физика радиационных повреждений и радиационное материаловедение»*. 2016, №2 (102), с. 25-32.

Article received 22.02.2017

ПРИМЕНЕНИЕ МОДЕЛЕЙ ВОДОРОДНОГО ОХРУПЧИВАНИЯ ПРИ АНАЛИЗЕ ЗАКОНОМЕРНОСТИ РОСТА БЛИСТЕРОВ В СТАЛИ 12Cr2MoNbVB И α-Fe, ОБЛУЧЕННЫХ НИЗКОЭНЕРГЕТИЧЕСКОЙ ДЕЙТЕРИЕВОЙ ПЛАЗМОЙ

А.В. Никитин, Г.Д. Толстолуцкая, В.В. Ружицкий, И.Е. Копанец, С.А. Карпов, Р.Л. Василенко, Г.Ю. Ростова, Н.Д. Рыбальченко, Б.С. Сунгуров

Исследованы процессы развития блистеров и связанных с ними подповерхностных трещин, возникающих при воздействии при различных температурах на 12Cr2MoNbVB ферритно-мартенситную сталь и α-Fe водородной плазмы тлеющего разряда с энергией ионов ~ 1 кэВ и дозой ~ $2\cdot10^{24}$ D/м^2. Использованы методы сканирующей электронной микроскопии, термодесорбции и ядерная реакция D(^{3}He, p)^{4}He. Получены температурные зависимости среднего диаметра блистеров, пространственное распределение дейтерия в объеме материала и температурные интервалы его удержания. Влияние водорода на развитие блистеринга рассмотрено с привлечением моделей, разработанных для водородного охрупчивания материалов. На основе этого анализа сделан вывод, что значительные темпы роста трещин и блистеров могут возникать во время периодов отключения реактора, когда температура конструкций снижается до 373 K.

ЗАСТОСУВАННЯ МОДЕЛЕЙ ВОДНЕВОГО ОКРИХЧЕННЯ ПРИ АНАЛІЗІ ЗАКОНОМІРНОСТІ РОСТУ БЛІСТЕРІВ У СТАЛІ 12Cr2MoNbVB І α-Fe, ОПРОМІНЕНИХ НИЗЬКОЕНЕРГЕТИЧНОЮ ДЕЙТЕРІЄВОЮ ПЛАЗМОЮ

А.В. Нікітін, Г.Д. Толстолуцька, В.В. Ружицький, І.Є. Копанець, С.О. Карпов, Р.Л. Василенко, Г.Ю. Ростова, Н.Д. Рибальченко, Б.С. Сунгуров

Досліджено процеси розвитку блістерів і пов'язаних з ними підповерхневих тріщин, що виникають при впливі при різних температурах на 12Cr2MoNbVB феритно-мартенситну сталь і α-Fe водневої плазми тліючого розряду з енергією іонів ~ 1 кеВ і дозою ~ $2\cdot10^{24}$ D/м^2. Використано методи скануючої електронної мікроскопії, термодесорбції і ядерна реакція D(^{3}He, p)^{4}He. Отримано температурні залежності середнього діаметра блістерів, просторовий розподіл дейтерію в обсязі матеріалу і температурні інтервали його утримання. Вплив водню на розвиток блістерінга розглянуто із залученням моделей, розроблених для водневого охрихчення матеріалів. На основі цього аналізу зроблено висновок, що значні темпи зростання тріщин і блістерів можуть виникати під час періодів відключення реактора, коли температура конструкцій знижується до 373 K.